Applied Surface Science 365 (2016) 160–165

Contents lists available at ScienceDirect

Applied Surface Science

journal homepage: www.elsevier.com/locate/apsusc

Wafer-scale, conformal and direct growth of MoS_2 thin films by atomic layer deposition

Yujin Jang[a,b], Seungmin Yeo[c], Han-Bo-Ram Lee[d], Hyungjun Kim[c], Soo-Hyun Kim[a,*]

[a] School of Materials Science and Engineering, Yeungnam University, Gyeongsangbuk-do 712-749, Republic of Korea
[b] Busan Center, Korea Basic Science Institute, 1275 Jisadong, Gangseogu, Busan 618-230, Republic of Korea
[c] School of Electrical Engineering, Yonsei University, 50 Yonsei-Ro, Seodaemun-Gu, Seoul 120-749, Republic of Korea
[d] Department of Materials Science and Engineering, Incheon National University, 119 Academi-ro, Yeonsu-gu, Incheon 406-772, Republic of Korea

ARTICLE INFO

Article history:
Received 2 October 2015
Received in revised form 3 January 2016
Accepted 7 January 2016
Available online 8 January 2016

Keywords:
MoS_2
Atomic layer deposition
$Mo(CO)_6$
H_2S plasma
Step coverage

ABSTRACT

Molybdenum disulfide (MoS_2) thin films were grown directly on SiO_2 covered wafers by atomic layer deposition (ALD) at the deposition temperatures ranging from 175 to 225 °C using molybdenum hexacarbonyl [$Mo(CO)_6$] and H_2S plasma as the precursor and reactant, respectively. Self-limited film growth on the thermally-grown SiO_2 substrate was observed with both the precursor and reactant pulsing time. The growth rate was ~0.05 nm/cycle and a short incubation cycle of around 13 was observed at a deposition temperature of 175 °C. The MoS_2 films formed nanocrystalline microstructure with a hexagonal crystal system (2H-MoS_2), which was confirmed by X-ray diffraction and transmission electron microscopy. Single crystal MoS_2 nanosheets, ~20 nm in size, were fabricated by controlling the number of ALD cycles. The ALD-MoS_2 thin films exhibited good stoichiometry with negligible C impurities, approximately 0.1 at.% from Rutherford backscattering spectrometry (RBS). X-ray photoelectron spectroscopy confirmed the formation of chemical bonding from MoS_2. The step coverage of ALD-MoS_2 was approximately 75% at a 100 nm sized trench. Overall, the ALD-MoS_2 process made uniform deposition possible on the wafer-scale (4 in. in diameter).

1. Introduction

Molybdenum disulfide (MoS_2) films have been traditionally known as a solid lubricant for tribological applications in high temperature and vacuum environments [1,2] and catalysis [3,4]. These MoS_2 films have been prepared by sputtering from a MoS_2 target [5–8] and chemical vapor deposition (CVD) [9–11] using various Mo and S containing metalorganic precursor of tert-butyl thiolate $Mo(S\text{-}t\text{-}Bu)_4$ [9] or the reaction of inorganic precursors, molybdenum hexafluoride (MoF_6) and molybdenum pentachloride ($MoCl_5$), with H_2S [11]. Recently, the significance of two dimensional materials has been manifested by the discovery of graphene. Among them, molybdenum disulfide is particularly interesting. In layered structures, each layer typically has a thickness of 6–7 Å, which consists of a hexagonally packed layer of molybdenum atoms sandwiched between two layers of sulfur atoms [12]. Bulk MoS_2 has an indirect band gap of 1.2 eV, whereas monolayer MoS_2 is a direct band gap semiconductor with a band gap of 1.8 eV [13]. In addition, MoS_2 monolayers have been reported to exhibit an excellent on/off current ratio of 1×10^8 and high carrier mobility of 168 $cm^2\,V^{-1}\,S^{-1}$ at 4 K to 60 $cm^2\,V^{-1}\,S^{-1}$ at 250 K [14]. The presence of a direct band gap in single layer MoS_2 makes it very interesting for applications, such as transistors [14–16], lithium ion batteries [17,18], amplifier devices [19], chemical sensors [20,21], and integrated circuits.

Significant efforts have been devoted to the preparation of monolayers or a few layers of MoS_2, including scotch tape-assisted micromechanical exfoliation [14,22,23], chemically exfoliation [17,24,25], vapor solid growth [26], sulfurization of MoO_3 or Mo films [27,28], annealing $(NH_4)_2MoS_4$ films [29], and chemical vapor deposition [30–35]. Most of these processes have several limitations, such as difficulties in controlling the thickness and poor large-area uniformity and the need for high deposition temperature. Therefore, a new preparation method is needed for producing high-quality MoS_2 thin films, MoS_2 nanosheets by precisely controlling the thickness of MoS_2 thin films, and for obtaining the uniformity for fabricating devices in a large-sized wafer. To achieve those objectives, atomic layer deposition (ALD) can be a viable solution for the preparation of MoS_2 thin films and nanosheets onto those emerging applications because ALD can provide excellent conformality, digital controllability of the film thickness, and

* Corresponding author.
E-mail address: soohyun@ynu.ac.kr (S.-H. Kim).

http://dx.doi.org/10.1016/j.apsusc.2016.01.038
0169-4332/

perfect large-area uniformity owing to its inherent surface-saturated and self-limited reaction mechanisms. Despite its many advantages, very few studies [36,37] have examined ALD-MoS_2 processes. Tan et al. reported the deposition of ALD-MoS_2 films using $MoCl_5$ with H_2S at a deposition temperature of 300 °C. Jin et al. evaluated other chemical routes to ALD-MoS_2, where molybdenum hexacarbonyl [$Mo(CO)_6$] and dimethyldisulfide (CH_3SSCH_3, DMDS) as Mo and S precursor, respectively, were used. The deposition temperature was quite low and was varied from 60 to 140 °C. Despite this, the film was deposited as an amorphous phase according to transmission electron microscopy (TEM) and X-ray diffraction (XRD).

In this study, crystalline and stoichiometric MoS_2 films were grown uniformly, reliably and directly on a wafer-scale (4 in. in diameter) without a post-sulfurization process by ALD using a $Mo(CO)_6$ precursor and H_2S plasma as the precursor and reactant, respectively. The growth kinetics of the ALD-MoS_2 process was also investigated with the deposition temperature ranging from 175 to 225 °C as well as their film properties. Based on the growth kinetics of ALD-MoS_2 process, single crystal MoS_2 nanosheets could also be prepared by controlling the number of ALD cycles.

2. Experiments

The MoS_2 film were deposited using a showerhead-type ALD (ALD) reactor (Lucida-M100, NCD Technology) with $Mo(CO)_6$ and H_2S plasma as the precursor and reactant, respectively. The precursor was a white powder at room temperature with a vapor pressure for 0.8 Torr at 40 °C. The deposition temperature was varied from 175 to 225 °C and the chamber pressure was fixed to 0.5 Torr, regardless of deposition temperature. The MoS_2 films were deposited on thermally grown SiO_2, single crystal GaN, and sapphire substrates. The Mo precursor was vaporized in a bubbler at 40 °C and carried to the chamber by Ar gas at 50 standard cubic centimeters per minute (sccm). The line temperature for precursor delivery was kept at 60 °C to prevent condensation of the precursor. H_2S gas was delivered with a flow late of 50 sccm as a reactant for the Mo precursor. During reactant pulsing, a radio frequency (RF) power of 100 watts (W) was applied to the showerhead to ignite the corresponding plasma. After the precursor pulse and reactant pulse, a purge with 200 sccm of Ar was performed for 10 s.

The properties of the MoS_2 films were analyzed using the following techniques. The thickness of the MoS_2 film was determined by cross-sectional view TEM (XTEM, Tecnai F20 equipped with a 200 kV accelerating voltage and a field emission gun) analysis. The phase and crystallinity were confirmed using grazing-incidence angle (incident angle, $\theta = 3°$) X-ray diffraction (GIAXRD, PANalytical X'-pert PRO MRD with Cu Kα radiation at 1.5 kW) analysis. The film composition and impurities were measured by Rutherford backscattering spectrometry (RBS) using He^{++} ions with incident energy of 2 MeV. XPS (ESCALAP 250 XPS Spectrometer in Korea Basic Science Institute Busan, Korea) was performed to examine the chemical bonding of the MoS_2 films. The optical properties were analyzed by UV–vis–NIR spectrophotometry (Cary 5000, Agilent Technologies). Plan-view bright field and high-resolution TEM were also used to examine the microstructure of MoS_2 films. The step coverage of the films was evaluated at the trench with a top opening width of 100 nm using XTEM analysis.

3. Results and discussion

First, the thermal decomposition of the Mo precursor was checked. For 20 min, the precursor was provided only to the substrate at various temperatures and it was found that until 225 °C, deposition did not occur but when the substrate temperature was increased to 250 °C, indicating the thermal decomposition of the precursor at this temperature. Therefore, the deposition temperature was controlled to be less than 250 °C.

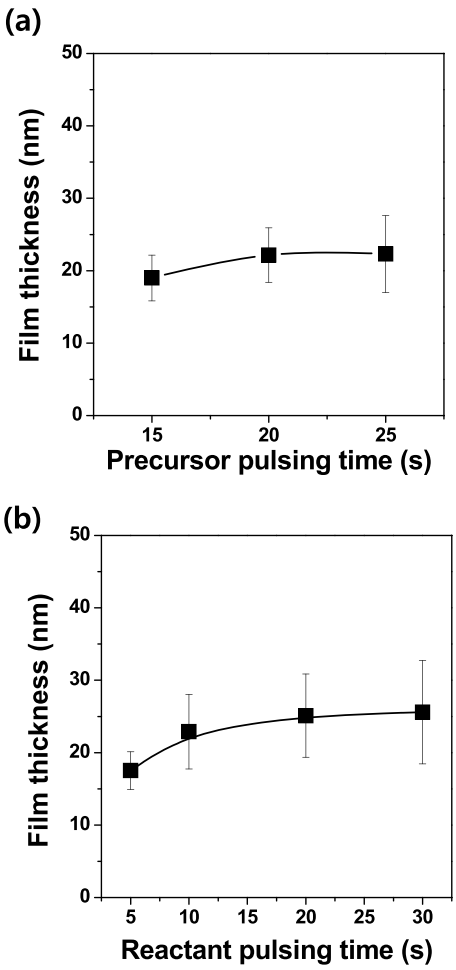

Fig. 1. Thicknesses of the films deposited on a thermally grown SiO_2 surface after 300 ALD cycles as a function of (a) Mo precursor pulsing time and (b) reactant (H_2S plasma) pulsing time. The reactant pulsing time was fixed to 20 s for (a) and the precursor pulsing time was 10 s for (b).

Self-limited film growth behavior was identified at a deposition temperature of 175 °C with the number of reaction cycles fixed to 500. Fig. 1(a) and (b) shows the growth kinetics with precursor pulsing time and reactant pulsing time. Fig. 1(a) shows the thickness of the MoS_2 thin films deposited on thermally grown SiO_2 substrates as a function of the precursor pulsing time, which was varied from 15 to 25 s at a fixed reactant pulsing time of 10 s. With increasing precursor pulsing time from 15 to 20 s, the film thickness was slightly increased. The film thickness did not increase with further increases in the precursor pulsing time to 25 s. For precursor pulsing times of more than 20 s, the films thickness appeared to become saturated. Similar growth behavior was observed when the H_2S gas pulsing time was varied from 5 to 30 s, as shown in Fig. 1(b). In the case of the reactant pulsing time, the film was saturated after a 10 s pulsing time. Therefore, from Fig. 1(a) and (b), the basic pulsing conditions was determined to be a precursor pulsing time of 20 s, precursor purging time of 10 s, reactant pulsing time of 10 s, and reactant purging time of 10 s.

Fig. 2 shows the thicknesses of MoS_2 films deposited on SiO_2 as a function of the number of ALD reaction cycles at a deposition temperature of 175 °C. Under basic pulsing conditions, the number of reaction cycles was varied from 100 to 600 cycles. The film thickness increased linearly with increasing number of reaction cycles.

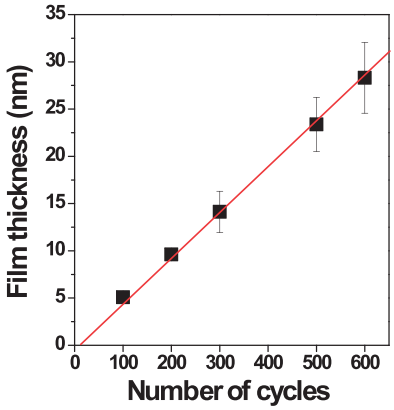

Fig. 2. Thickness of the ALD-MoS_2 films deposited under the basic pulsing conditions as a function of number of the ALD reaction cycles.

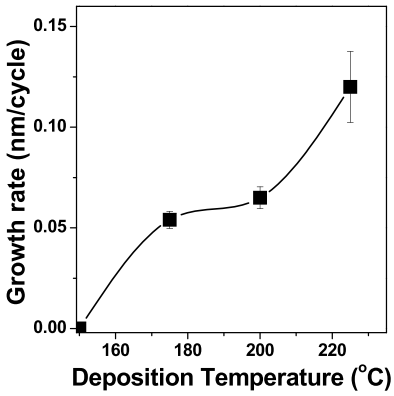

Fig. 3. Growth rate of ALD-MoS_2 films as a function of the deposition temperature.

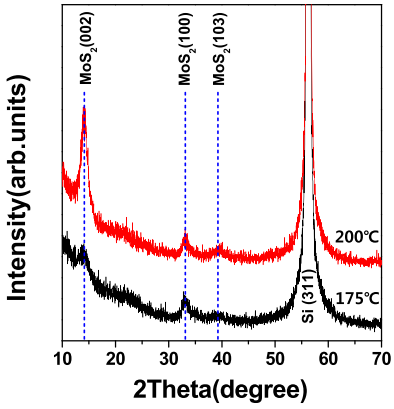

Fig. 4. GIAXRD analysis result on ALD-MoS_2 films with deposition temperature.

The growth rate on the SiO_2 substrate, as determined by linear fitting, was approximately 0.05 nm/cycle. The number of incubation cycles was approximately 13 cycles from a linear fit of the data. Compared to previous reports on ALD-MoS_2, the growth rate of the present process was lower. The growth rate of ALD-MoS_2 deposited with $MoCl_5$ with H_2S at 300 °C was ~0.18 nm/cycle [36] and that deposited with $Mo(CO)_6$ and dimethyldisulfide at 100 °C was ~0.11 nm/cycle [37]. With increasing deposition temperature to 140 °C, the growth rate was increased significantly to ~0.25 nm/cycle for ALD-MoS_2 using $Mo(CO)_6$ and dimethyldisulfide. This suggests that the growth rate of ALD-MoS_2 process depends on the precursor and reactant used as well as the deposition temperature.

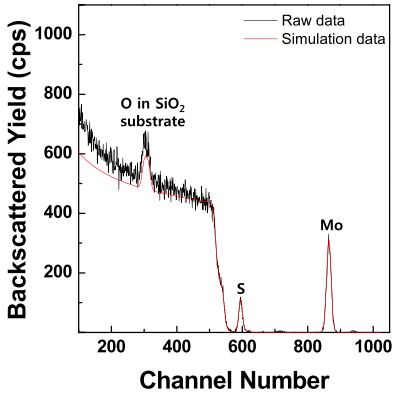

Fig. 5. RBS spectra of the ALD-MoS_2 films deposited on a SiO_2 (100 nm in thickness)-covered Si wafer at 200 °C with incident He^{++} energies of 2 MeV.

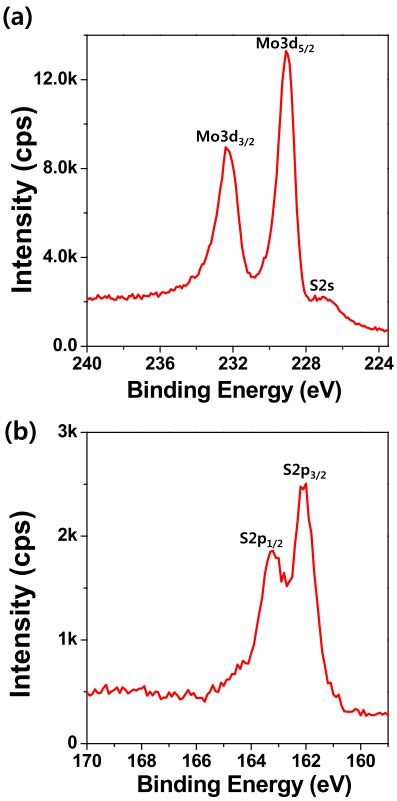

Fig. 6. XPS spectra of the ALD-MoS_2 films: (a) Mo 3*d* and (b) S 2*p* spectra.

Fig. 3 shows the growth rate of the MoS_2 film as a function of the deposition temperature under basic pulsing conditions. The deposition temperatures were varied from 150 to 225 °C but film growth did not occur at 150 °C. At temperatures from 175 to 200 °C, the growth rate was relatively constant. On the other hand, when the deposition temperature was increased further to 225 °C, the growth rate again increased rapidly to approximately 0.12 nm/cycles due to partial decomposition of the precursor. Therefore, the ALD temperature window of between 175 and 200 °C for the growth of ALD-MoS_2 using Mo hexacarbonyl and H_2S plasma was confirmed. In this temperature range, the growth rate was relatively constant and the growth rate was approximately 0.05 nm/cycle.

Fig. 4 shows the grazing incidence angle ($\theta = 3°$) XRD patterns of the MoS_2 films deposited at a deposition temperature of 175 and 200 °C with the ALD cycles of 300. Here, the film thickness was similar, ~15 nm. For both MoS_2 films, three peaks [(0 0 2),

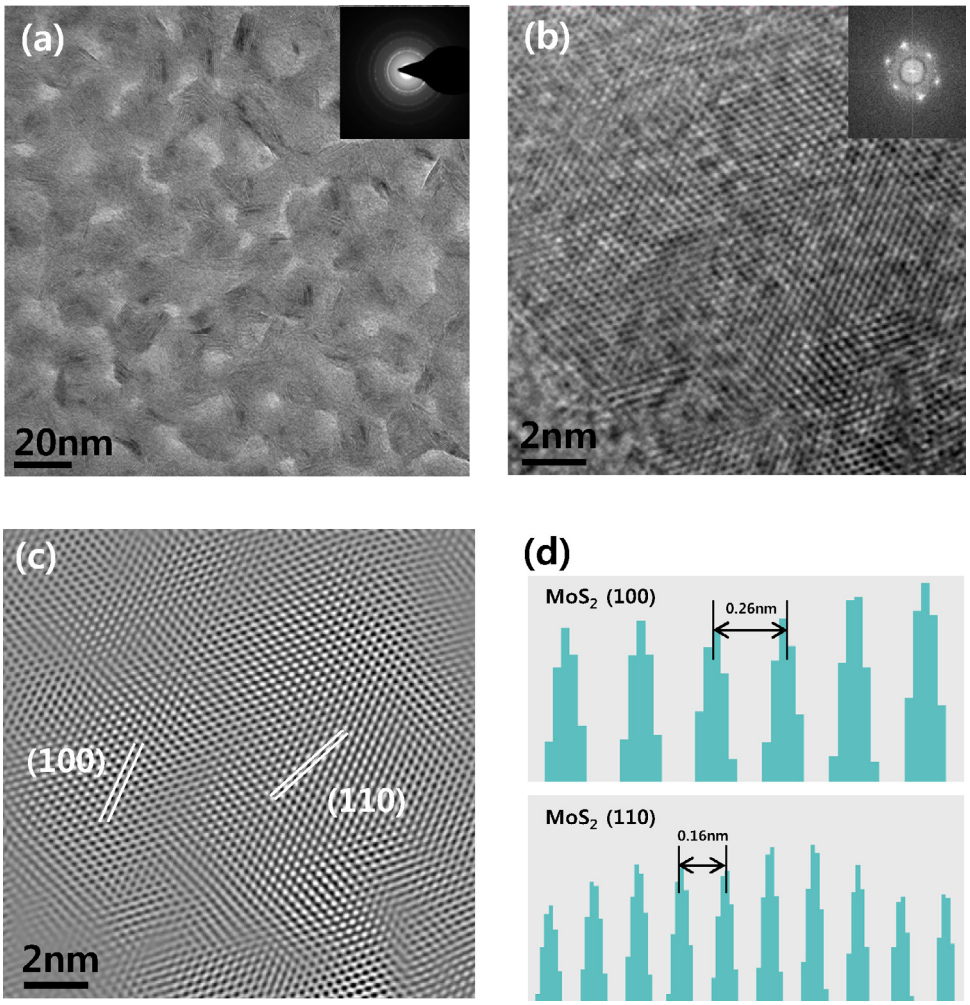

Fig. 7. Plan-view TEM image of ALD-MoS_2 films: (a) bright-field image of ALD-MoS_2 film deposited on SiO_2 (the inset shows the SAD pattern of the film), (b) high resolution (HR) image, (c) the constructed HR image from the Fourier transformation of the real HR image, and (d) the line profile showing the layer spacing in (c).

14.378° 2θ; (1 0 0), 32.677° 2θ; and (1 0 3), 39.539° 2θ] from 2H-MoS_2 phase where each Mo atom is prismatically coordinated by six surrounding S atoms, were clearly observed, indicating that the MoS_2 film forms a polycrystalline structure. Fig. 4 also shows that the intensities of the XRD peaks increased with increasing deposition temperature, suggesting that increasing the deposition temperature improved the film crystallinity.

The film composition was measured by RBS analysis. Fig. 5 showed the RBS spectra of the MoS_2 film deposited on the SiO_2 substrate, where the incident He^{++} energy is 2.0 MeV. The He^{++} ions backscattered from a collision with Mo and S atoms in the films are shown at the channel number at approximately ~860 and ~600, respectively. Backscattered peaks from Si consist of 2 different positions. The first peak is at a channel number of ~530, which is the backscattered one from Si in the thermally grown SiO_2. In addition, the backscattered peak from Si in the Si wafer was observed at a channel number of ~500 with the highest yield. The backscattered peak shown at a channel number of ~300 was from O in the SiO_2. The backscattered peak related to O in MoS_2 film, which should be shown at higher channel numbers than ~300 (or higher backscattered He^{++} energy) was not detected as well as that related to C in MoS_2 film were not detected from RBS. Using a RUMP simulation for RBS analysis, the film composition was determined to be $MoS_{2.2}$, which closely matched the XRD results showing the formation of a 2H-MoS_2 phase. The formation of almost pure and stoichiometric MoS_2 using the present ALD scheme was notable considering that even sputter-deposited MoS_2 films contained oxygen or carbon impurities of approximately 8 at.% [5,6] and CVD-MoS_2 film also contained 6 at.% carbon and 3 at.% oxygen [9]. Therefore, the RBS results suggested that the ALD-MoS_2 process examined in this study could have advantages in terms of film stoichiometry and purity.

The films deposited under the basic pulsing conditions were analyzed by XPS to determine the chemical bonding configuration. The XPS data was obtained after sputtering an approximately 10-nm-thick film at the surface to exclude C and O contamination and to characterize the bonding status of the film itself. The XPS data was calibrated to the adventitious C 1*s* peak detected on the film surface. Fig. 6(a) shows the spectrum of the Mo 3*d* photoelectrons. The most intensive peak centered at approximately 229 eV was assigned to the Mo—S bonding to form 2H-MoS_2 (Mo $3d_{5/2}$: 229 eV) [24]. The second intensive peak centered at approximately 232.3 eV could be also due to the Mo—S bonding to form 2H-MoS_2 (Mo $3d_{3/2}$: 232 eV). The broad peak centered at approximately 226.8 eV was a S-related XPS peak not a Mo-related XPS one [38]. The binding energy peak related to the bonding with Mo and O, which is shown at ~235 eV, was not shown, indicating that the MoS_2 film does not contain the oxygen impurities, which is the same result with RBS analysis. Fig. 6(b) shows the spectrum of S 2*p* photoelectrons. Two intensive peaks were clearly observed at 162.1 and 163.2 eV, which could be identified as S $2p_{3/2}$ and S $2p_{1/2}$, respectively, and are related to S—Mo boding to form 2H-MoS_2 [24].

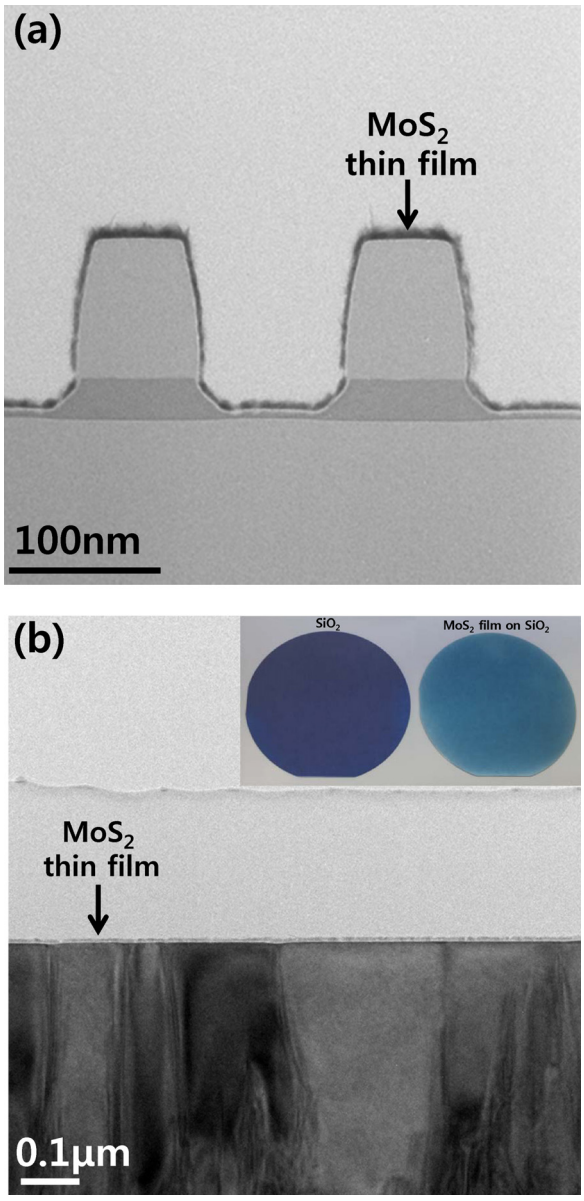

Fig. 8. (a) XTEM image showing step coverage of the ALD-MoS_2 film over the nano-scale trenches structure and (b) the large-area uniform growth of ALD-MoS_2 film (the inset figure shows the ALD-MoS_2 thin film grown in a 4 in.-diameter wafer).

TEM images shown in Fig. 7(a)–(c) confirmed the phase and characterized the microstructure of the MoS_2 film in details. The plan-view TEM bright-field (BF) image of the MoS_2 film deposited on SiO_2 substrate with 100 ALD cycles shows poly-crystalline grains with sizes ranging from 15 to 20 nm. The corresponding selected-area electron diffraction (SAED) pattern (inset) was matched with that of the 2H-MoS_2, which is consistent with the XRD results. MoS_2 single crystalline nanosheets could be prepared by controlling the number of ALD cycles, as shown by Fig. 7(b). Fig. 7(b) presents a plan-view TEM high resolution (HR) image of MoS_2 deposited with 30 ALD cycles. A honeycomb-like structure and 6-fold coordination symmetry were observed and the fast Fourier transformation [inset in Fig. 7(b)] clearly showed a spot pattern in reciprocal space, indicating the formation of a single crystal with a size of ~20 nm. The grain size of single crystal nanosheet from this study was significantly lower than those from mechanical exfoliation and CVD method, which showed the grain sizes of several μm [14,21,31–33]. To extract the lattice spacing and crystal direction precisely, inverse fast Fourier transformation was performed by applying a mask to the inset figure in Fig. 7(b) using the Gatan Digital Micrograph software package, leading to a constructed HR image [Fig. 7(c)]. From the constructed HR image, the lattice spacing in each direction was determined from the intensity profile [Fig. 7(d)], and was 0.26 nm and 0.16 nm for the (1 0 0) and (1 1 0) planes, respectively.

Fig. 8(a) shows the cross-section TEM (XTEM) images of the overall trenches (top opening width of ~100 nm) coated with the ALD-MoS_2 layer grown under the basic pulsing conditions. The XTEM images clearly show that the ALD-MoS_2 film was coated conformally and uniformly over the surface of the nano-scale trenches. The thicknesses of the ALD-MoS_2 film at the top, middle, and bottom of the trench were approximately 10.0, 5.0 and 7.5 nm, indicating ~75% bottom coverage. The good step coverage on these nano-scale trenches shows that the MoS_2 film can be deposited under ideal ALD growth mode without partial decomposition of the precursor. Fig. 8(b) shows XTEM images of the MoS_2 films grown on a single crystal GaN substrate. The XTEM image clearly showed that the 5 nm-thick ALD-MoS_2 films could be grown very uniformly in a large region and TEM observations were possible (~1 μm). In addition, the inset figure clearly shows that the MoS_2 film (20 nm in thickness) was grown uniformly on a SiO_2 covered Si wafer (4 in. in diameter).

4. Summary and conclusion

Highly conformal MoS_2 thin films were deposited by ALD using a $Mo(CO)_6$ and H_2S plasma as the precursor and reactant on a 4 in. diameter wafer from 175 to 225 °C, and their physical properties were investigated. The ALD window temperature was observed between 175 and 200 °C. Self-limiting film growth was observed with both the precursor and reactant pulsing time, and the growth rate on the thermally-grown SiO_2 substrate was approximately 0.05 nm/cycle and a short incubation cycle of approximately 13 was observed at a deposition temperature of 175 °C. Owing to the inherent advantages of the ALD process, the film thickness could be controlled precisely and single crystal MoS_2 nanosheets could be prepared by controlling the number of ALD cycles. The ALD-MoS_2 thin films were quite stoichiometric and pure with negligible impurities, such as C and O in the film according to RBS and XPS. The step coverage of MoS_2 was excellent at approximately 75% at a 100 nm sized trench and wafer-scale growth (4 in. in diameter) was demonstrated. In conclusion, the ALD-MoS_2 process developed in this study could be a viable solution for preparing MoS_2 nanosheets and thin films reliably and uniformly for various applications, such as catalysts, electronic devices and sensors.

Acknowledgments

This study (2015R1A2A2A04004945) was supported by the Mid-career Researcher Program through NRF grant funded by the MEST and also partially supported by the Human Resource Training Program for Regional Innovation and Creativity through the Ministry of Education and NRF, Korea (NRF-2014H1C1A1066809) and Human Resources Program in the Transportation Specialized Lighting Core Technology Development granted financial resource from the Ministry of Trade, Industry and Energy (No. N0001364).

References

[1] M.R. Hilton, R. Bauer, P.D. Fleischauer, Tribological performance and deformation of sputter-deposited MoS_2 solid lubricant films during sliding ware and indentation contact, Thin Solid Films 188 (1990) 219–236.
[2] M.R. Hilton, R. Bauer, S.V. Didziulis, M.T. Dugger, J.M. Keem, J. Scholhamer, Structural and tribological studied of MoS_2 solid lubricant films having tailored metal-multilayer nanostructures, Surf. Coat. Technol. 53 (1992) 13–23.

[3] S.K. Srivastava, B.N. Avasthi, Preparation and characterization of molybdenum disulphide catalysts, J. Mater. Sci. 28 (1993) 5032–5035.
[4] P. Faye, E. Payen, D. Bougeard, Cluster approach of active sites in an MoS_2 catalyst, J. Mol. Model. 5 (1999) 63–71.
[5] J.R. Lince, P.D. Flischauer, Crystallinity of rf-sputtered MoS_2 films, J. Mater. Res. 2 (6) (1987) 827–838.
[6] P.A. Bertrand, Orientation of re-sputter-deposited MoS_2 films, J. Mater. Res. 4 (1) (1989) 180–184.
[7] M.R. Hilron, P.D. Flischauer, TEM lattice imaging of the nanostructure of early-growth sputter-deposited MoS_2 solid lubricant films, J. Mater. Res. 5 (2) (1990) 406–421.
[8] C. Muratore, A.A. Voevodin, Control of molybdenum disulfide basal plane orientation during coating growth in pulsed magnetron sputtering discharges, Thin Solid Films 517 (19) (2009) 5605–5610.
[9] J. Cheon, J.E. Gozum, G.S. Girolami, Chemical vapor deposition of MoS_2 and TiS_2 films from metal-organic precursor $Mo(S\text{-}t\text{-}Bu)_4$ and $Ti(S\text{-}t\text{-}Bu)_4$, Chem. Mater. 9 (1997) 1847–1853.
[10] W.K. Hofmann, Thin films of molybdenum and tungsten disulphides by metal organic chemical vapor deposition, J. Mater. Sci. 23 (1988) 3981–3986.
[11] W.Y. Lee, T.M. Beamann, M.W. Stott, Preparation of MoS_2 thin films by chemical vapor deposition, J. Mater. Res. 9 (6) (1994) 1475–1483.
[12] Q.H. Wang, K.K. Kalantal-Zadeh, A. Kis, J.N. Coleman, M.S. Strano, Electronics and optoelectronics of two-dimensional transition metal dichalcogenides, Nat. Nanotechnol. 7 (2012) 699–712.
[13] J. Qi, X. Li, X. Qian, J. Feng, Bandgap engineering of rippled MoS_2 monolayer under external electric field, J. Appl. Phys. Lett. 102 (17) (2013) 173112.
[14] B. Radisavl Jevic, A. Radenovic, J. Brivio, V. Giacometti, A. Kis, Single-layer MoS_2 transistors, Nat. Nanotechnol. 6 (2011) 147–150.
[15] R.A. Street, Thin-film transistors, Adv. Mater. 21 (2009) 2007–2022.
[16] S. Ghatak, A.N. Pal, A. Ghosh, Nature of electronic states in atomically thin MoS_2 field-effect transistors, ACS Nano 5 (10) (2011) 7707–7712.
[17] J. Xiao, D. Choi, L. Cosimbescu, P. Koech, J. Liu, J.P. Lemmon, Exfoliated MoS_2 nanocomposite as an anode material for lithium ion batteries, Chem. Mater. 22 (2010) 4522–4524.
[18] Y. Shi, Y. Wang, J.I. Wong, A.Y.S. Tan, C. Hsu, L. Li, Y. Lu, H.Y. Yang, Self-assembly of hierarchical MoS_x/CNT nanocomposites ($2 < x < 3$): towards high performance anode materials for lithium ion batteries, Sci. Rep. 3 (2013).
[19] B. Radisavl Jevic, M.B. Whitwick, A. Kis, Small-signal amplifier cased on single-layer MoS_2, Appl. Phys. Lett. 101 (4) (2012) 043103.
[20] F.K. Perkins, A.L. Friedman, E. Cobas, P.M. Campbell, G.G. Jernigan, B.T. Jonker, Chemical vapor sensing with monolayer MoS_2, Nano Lett. 13 (2013) 668–673.
[21] D.J. Late, Y. Huang, B. Liu, J. Acharya, S.N. Shirodkar, J. Luo, A. Yan, D. Charles, U.V. Waghmare, V.P. Dravid, C.N.R. Rao, Sensing behavior of atomically thin-layered MoS_2 transistors, ACS Nano 7 (6) (2013) 4879–4891.
[22] A. Splendiani, L. Sun, Y. Zhang, T. Li, J. Kim, C.Y. Chim, G. Galli, F. Wang, Emerging photoluminescence in monolayer MoS_2, Nano Lett. 10 (4) (2010) 1271–1275.
[23] K.S. Novoselov, D. Jiang, F. Schedin, T. Booth, V.V. Khotkevich, S.V. Morozov, A.K. Geim, Two-dimensional atomic crystals, Proc. Natl. Acad. Sci. U.S.A. 102 (30) (2005) 10451–10453.
[24] G. Eda, H. Yamaguchi, D. Voiry, T. Fugita, M. Chen, M. Chhowalla, Photoluminescence from chemically exfoliated MoS_2, Nano Lett. 11 (2011) 5111–5116.
[25] J.N. Coleman, M. Lotya, A. O'Neill, S.D. Bergin, P.J. King, U. Khan, K. Young, A. Gaucher, S. De, R.J. Smith, I.V. Shvets, S.K. Arora, G. Stanton, H. Kim, K. Lee, G.T. Kim, G.S. Deusberg, T. Hallam, J.J. Bolang, J.J. Wang, J.F. Donegan, J.C. Grunlan, G. Moriarty, A. Shmeliov, R.J. Nichollos, P.D. Nellist, V. Nicolosi, Two-dimensional nanosheets produced by liquid exfoliation of layered materials, Science 331 (6017) (2011) 568–571.
[26] S. Wu, C. Huang, G. Aivazian, J.S. Ross, D.H. Cobden, X. Xu, Vapor–solid growth of high optical quality MoS_2 monolayers with near-unity valley polarization, ACS Nano 7 (3) (2013) 2768–2772.
[27] Y. Zhan, Z. Liu, S. Najmaei, P.M. Ajayan, J. Lou, Large area vapor phase growth and characterization of MoS_2 atomic layers on SiO_2 substrate, Small 8 (7) (2012) 966–971.
[28] Y.C. Lin, W. Zhang, J.K. Huang, K.K. Liu, Y.H. Lee, C.T. Liang, C.W. Chu, L.J. Li, Wafer-scale MoS_2 thin layers prepared by MoO_3 sulfurization, Nanoscale 4 (20) (2012) 6637–6641.
[29] K.K. Liu, W. Zhang, Y.H. Lee, Y.C. Lin, M.T. Chang, C.Y. Su, C.S. Chang, H. Li, Y. Shi, H. Zhang, C.S. Lai, L.J. Li, Growth of large-area and highly crystalline MoS_2 thin layers on insulating substrates, Nano Lett. 12 (3) (2012) 1538–1544.
[30] Y.H. Lee, X.Q. Zhang, W. Zhang, M.T. Chang, C.T. Lin, K.D. Chang, Y.C. Yu, J.T.W. Wang, C.S. Chang, L.J. Li, T.W. Lin, Synthesis of large-area MoS_2 atomic layers with chemical vapor deposition, Adv. Mater. 24 (2012) 2320–2325.
[31] Y.H. Lee, L. Yu, H. Wang, W. Fang, X. Ling, Y. Shi, C.H. Lin, J.K. Huang, M.T. Chang, C.S. Chang, M. Dreerlhaus, T. Palasios, L.J. Li, J. Kong, Synthesis and transfer of single-layer transition metal disulfides on diverse surface, Nano Lett. 13 (4) (2013) 1852–1857.
[32] Y. Yu, C. Li, Y. Liu, L. Su, Y. Zhang, L. Cao, Controlled scalable synthesis of uniform, high-quality monolayer and few-layer MoS_2 films, Sci. Rep. 3 (2013).
[33] S. Najmael, Z. Liu, W. Zhou, X. Zou, G. Shi, S. Lei, B.I. Yakocson, J.C. Idrobo, P.M. Ajayan, J. Lou, Vapor phase growth and grain boundary structure of molybdenum disulphide atomic layers, Nat. Mater. 12 (8) (2013) 754–759.
[34] A.M. Zande, P.Y. Huang, D.A. Chenet, T.C. Berkerlbach, Y.M. You, G.H. Lee, T.F. Heinz, D.R. Reichman, D.A. Muller, J.C. Hong, Grains and grain boundaries in highly crystalline monolayer molybdenum disulphide, Nat. Mater. 12 (6) (2013) 554–561.
[35] W. Wu, D. De, S.C. Chang, Y. Wang, H. Peng, J. Bao, S.S. Pei, High mobility and high on/off ratio field-effect transistors based on chemical vapor deposited single-crystal MoS_2 grains, Appl. Phys. Lett. 102 (14) (2013) 142106.
[36] L.K. Tan, B. Liu, J.H. Teng, S. Guo, H.Y. Low, K.P. Loh, Atomic layer deposition of a MoS_2 film, Nanoscale 6 (2014) 10584–10588.
[37] Z. Jin, S. Shin, D.H. Kwon, S.-J. Han, Y.-S. Min, Novel chemical route for atomic layer deposition of MoS_2 thin film on SiO_2/Si substrate, Nanoscale 6 (2014) 14453–14458.
[38] M.A. Baker, R. Gilmore, C. Lenardi, W. Gissler, XPS investigation of preferential sputtering of S from MoS_2 and determination of MoS_x stoichiometry from Mo and S peak positions, J. Appl. Surf. Sci. 150 (1999) 255–262.